

Dražen Jurišić, George S. Moschytz, Neven Mijat

Low-Sensitivity Active-RC Allpole Filters Using Optimized Biquads

UDK 621.372.63
IFAC 5.5.4

Original scientific paper

In this paper we present an optimal design procedure for second- and third-order active resistance-capacitance (RC) single-amplifier building blocks that are used to build a high-order tolerance-insensitive allpole filter. The design procedure of low-sensitivity, low-pass second- and third-order active-RC allpole filters, with positive feedback, has already been published. The design was extended to the high-pass and band-pass filters, as well as, to the filters using negative feedback. In this paper we summarize all these previously presented designs in the form of a tabulated step-by-step design framework (cookbook). The low passive sensitivity of the resulting circuits, as well as low active sensitivity features are demonstrated on the high-order Chebyshev filter examples. The resulting low passive sensitivity is investigated using the Schoeffler sensitivity measure, whereas the low active sensitivity is investigated with Matlab using finite and frequency dependent opamp gain.

Key words: Low-sensitivity active-RC filters, Single-amplifier biquads and bitriplets, Cascade design

Projektiranje svepolnih aktivnih RC filtara niske osjetljivosti pomoću optimiranih bikvadratnih sekcija. Prikazan je optimalan postupak projektiranja aktivnih RC filtarskih sekcija drugog i trećeg reda bez konačnih nula s jednim pojačalom koje se koriste pri građenju filtara visokog reda s niskom osjetljivošću. Postupak projektiranja nisko osjetljivih, nisko propusnih filtara već je objavljen, a u ovome je radu navedeni postupak proširen na nove sekcije koje realiziraju pojasno propusnu i visoko propusnu frekvencijsku karakteristiku kao i na sekcije koje koriste negativnu povratnu vezu u realizaciji. Svi su postupci optimalnog projektiranja sažeti i raspoloživi u obliku tablica s postupkom projektiranja “korak po korak”. Niska osjetljivost na tolerancije pasivnih komponenata, kao i niska osjetljivost na varijacije aktivnog elementa (pojačala) pokazani su na primjerima projektiranja Chebyshev-ljevih filtara visokog reda. Pritom ostvarena niska osjetljivost, kako pasivna tako i aktivna, istraživane su pomoću Shefflerove mjere osjetljivosti, odnosno uporabom frekvencijski ovisnog modela operacijskog pojačala u simulaciji pomoću programa Matlab.

Ključne riječi: aktivni RC filtri, niska osjetljivost, bikvadratne sekcije s jednim pojačalom, kaskadna struktura

1 INTRODUCTION

In this paper, a method of designing high-order allpole active-RC filters (both even and odd order) using combination of second- and third-order single-amplifier filter sections (*bi-quads* and, for lack of a better word, *bi-triplets*) is presented. Second- and third-order building blocks are designed in an optimal way and can be used in the cascade or some other structure of high-order filters.

To keep the cost of the filters low, it is desirable to avoid the need for filter tuning, and this is possible only for filters of medium to low selectivity and low sensitivity to component tolerances. Fortunately the RC ladder nature of the resulting circuits permits a recently introduced scheme of *impedance tapering* [1] which in many cases can reduce the sensitivity to component tolerances sufficiently to eliminate the need for tuning. Furthermore, the perfor-

mance of the filters when they operate on high frequencies can be improved by reducing their active sensitivity, and by that reducing the influence of the finite gain-bandwidth product (GBW) of a real operational amplifier (opamp). Active sensitivity reduction is accomplished by the gain-sensitivity product (GSP) minimization. The reduction of active sensitivity is performed together with reduction of passive sensitivity.

Preliminary results of the new design method have been presented elsewhere [1–5] for filters of second- and third-order and for low-pass (LP), band-pass (BP) and high-pass (HP) filter types. For those filters, sensitivity to component tolerance, which is considered one of the main performance criteria, was investigated in detail. The sensitivity of a filter transfer function to passive component tolerances is examined using the Schoeffler sensitivity measure as a

basis for comparison [6]. Using Matlab with real opamp model, having the finite GBW product, the filter performance at high frequency is simulated and by that the active sensitivity is investigated.

In Section 2 the main idea how to design low-sensitivity filters is explained. In Sections 3 and 4, a complete step-by-step design procedure for the most common LP, BP and HP filters of the second- and third-order is summarized in the form of a cookbook (table). Although no cookbook approach will solve all possible problems, it is often preferable to use quick step-by-step designs instead of returning to complicated equations to obtain slightly better performance. In the cookbook in this paper engineer uses tabulated equations and mechanically follows prescribed procedure. The most useful (recommended) filter sections are marked. In Section 3 it is also shown that HP filters have dual properties to LP filters in the sense of sensitivity and thus possess dual optimum design procedures. It is demonstrated that filters related by the complementary transformation have identical properties in the sense of sensitivity and thus possess identical optimum designs. The largest variety of biquads for realization of BP transfer function is presented.

In Section 5 the main features of our design procedure, namely, low passive and active sensitivities are illustrated by examples of seventh-order LP and HP, and sixth-order BP filters realized by cascading optimum biquads. The resulting optimized high-order cascaded filters are compared with other designs such as non-optimized cascade (designed simply by using equal caps and res).

2 LOW SENSITIVITY DESIGN

Consider the transfer function $T(s)$ of an n th-order allpole filter in terms of the transfer function coefficients:

$$T(s) = \frac{N(s)}{D(s)} = \frac{Kb_k s^k}{s^n + a_{n-1}s^{n-1} + \dots + a_i s^i + \dots + a_1 s + a_0}. \quad (1)$$

The transfer function $T(s)$ in (1) has no finite zeros, i.e. it has n zeros at infinity ($k=0$) for a LP filter, k -fold zero at the origin ($k=n/2$) for a BP filter, or $k=n$ for a HP filter. (For convenience we denote $b_0=a_0$ in (1) for LP filter.) In this paper we consider building blocks of the second- and third-order having transfer functions of the form (1) (with $n=2$ or 3). For the filters given in Figures 2–4, transfer function coefficients a_i are given in Tables 1, 3 and 5. In Tables 2, 4 and 6 the corresponding optimum designs are summarized in the form of a designer's cookbook.

The relative sensitivity of a function $F(x)$ to variations of a variable x is defined as

$$S_x^{F(x)} = \frac{dF/F}{dx/x} = \frac{dF(x)}{dx} \frac{x}{F(x)} = \frac{d[\ln F(x)]}{d[\ln x]}. \quad (2)$$

The relative change of the filter transfer function $T(s)$ in (1) due to the variation of its coefficients a_i is given by

$$\frac{\Delta T(s)}{T(s)} = \sum_{i=0}^n S_{a_i}^{T(s)} \frac{\Delta a_i}{a_i}, \quad (3)$$

where $S_{a_i}^{T(s)}$ are the *amplitude-to-coefficient sensitivities*. The variation of the amplitude response $\alpha(\omega)$ is given by

$$\Delta \alpha(\omega) = \sum_{i=0}^n \operatorname{Re} \left[S_{a_i}^{T(s)} \right] \Big|_{s=j\omega} \cdot \frac{\Delta a_i}{a_i} = \sum_{i=0}^n f_i(\omega) \frac{\Delta a_i}{a_i}. \quad (4)$$

The coefficient a_i relative change is given by

$$\frac{\Delta a_i}{a_i} = \sum_{\mu=1}^r S_{R_\mu}^{a_i} \frac{\Delta R_\mu}{R_\mu} + \sum_{\nu=1}^c S_{C_\nu}^{a_i} \frac{\Delta C_\nu}{C_\nu} + S_\beta^{a_i} \frac{\Delta \beta}{\beta}, \quad (5)$$

where R_μ are resistors, C_ν capacitors and β the feedback gain of an operational amplifier. The terms $S_x^{a_i}$ represent the *coefficient-to-component sensitivities*.

The magnitude $|T(j\omega)|$ of $T(s)$ in (1) depends only on the values of the coefficients a_i of the polynomial $D(s)$ and frequency ω . The functions $f_i(\omega)$ in (4) represent another form of amplitude-to-coefficient sensitivities in (3), and are dependent on the values of a_i and ω , as well. The amplitude-to-coefficient sensitivities are proportional to the pole Qs, meaning that the higher pole Qs results by higher sensitivities. Since the high-order filters have higher pole-Qs, the general rule should be to design filters with as low ripple and as low order as consistent with the filter specifications.

Unlike the *amplitude-to-coefficient sensitivities*, the *coefficient-to-component sensitivities* are dependent on the realization of the filter circuit and can be reduced by non-standard filter design such as *impedance tapering* shown in [1]. Consider a general passive-RC, n th-order ladder network presented in Figure 1. *Impedance tapering* is essentially impedance-scaling every successive stage of a ladder-like structure by an increasingly high power of a scaling factor. In other words we successively *scale* each section by an increasing amount, that is, ρ , ρ^2 , ρ^3 , etc., in order to isolate each section from the next.

Consequently, if we apply *ideal tapering* to the ladder network in Figure 1(a), we shall have the network

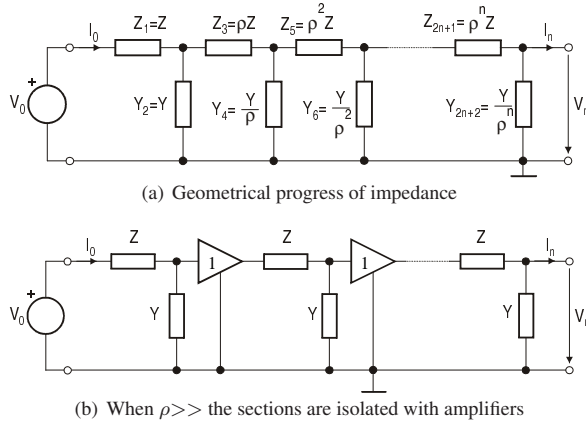


Fig. 1. Ideally impedance-tapered passive ladder network

presented in Figure 1(b). (The terms *ideal tapering* and *partial tapering* are used according to the definition in [1].) Note that, because of the geometrical progress of factor ρ , when ρ becomes high enough, the network can be represented with isolating amplifiers between adjacent L-sections. This is possible because impedance scaling of the middle L-section increases its input impedance and thus minimizes the loading of the previous L-section.

These successive increases of impedances reduce the coefficient-to-component sensitivities and by that reduce the overall transfer function sensitivity to component tolerances. In this paper, this design technique is applied to the most important practical second- and third-order building blocks (called *biquads* and *bitriplets*).

3 SECOND-ORDER BIQUADS

3.1 Second-order sections with positive feedback

Consider the second-order filters shown in Figure 2, having ladder-RC network in an opamp positive feedback loop. The circuits in Figure 2 belong to the Sallen and Key type [7]. The names of the filter sections are given according to [8, 9]. Transfer function has the form (1) with $n=2$ and the coefficients as function of components are in Table 1. The voltage gain β is obtained with an ideal non-inverting opamp and the gain is given by

$$\beta = 1 + R_F/R_G. \quad (6)$$

In what follows, we briefly demonstrate the desensitization on the example of HP filter circuit shown in Figure 2(b) [3, 4]. The sensitivities of the HP coefficient a_1 to all passive components $R_1, R_2, C_1, C_2, R_G,$ and R_F , given in [4] are repeated here:

$$\begin{aligned} S_{R_1}^{a_1} &= q_p \cdot \sqrt{\frac{R_2 C_2}{R_1 C_1}} (\beta - 1), \\ S_{R_2}^{a_1} &= -q_p \cdot \sqrt{\frac{R_1 C_1}{R_2 C_2}} \left(1 + \frac{C_2}{C_1}\right), \\ S_{C_1}^{a_1} &= q_p \cdot \sqrt{\frac{R_1 C_2}{R_2 C_1}} \left(\frac{R_2}{R_1} (\beta - 1) - 1\right), \\ S_{C_2}^{a_1} &= -q_p \cdot \sqrt{\frac{R_1 C_1}{R_2 C_2}}, \\ S_{R_G}^{a_1} &= S_{\beta}^{a_1} S_{R_G}^{\beta} = -S_{R_F}^{a_1} = \\ &= q_p \cdot \sqrt{(R_2 C_2)/(R_1 C_1)} (\beta - 1). \end{aligned} \quad (7)$$

Incidentally, it can be shown that the sum of the sensitivities (7) of a_1 to all resistors and also to all capacitors equals minus one, that is,

$$\sum_{\mu=1}^2 S_{R_{\mu}}^{a_1} = \sum_{\nu=1}^2 S_{C_{\nu}}^{a_1} = -1. \quad (8)$$

Expressions of this kind are often referred to as *sensitivity invariants*. They are a result of the so-called *homogeneity* of the function in question; in this case being the homogeneity of the coefficient $a_1(R_i, C_i)$.

Note that all sensitivities of the coefficient a_0 to passive components are equal to a theoretical minimum of $-1/2$ (and to the R_G and R_F they are zero). All good active filters should have gain-independent a_0 .

Thus, there is nothing that can be done to reduce a_0 sensitivities; but on the other hand, coefficient a_1 sensitivities in (7) depend on the component values.

The general impedance scaling factors, providing the relationship between elements in the RC network, are given by:

$$\begin{aligned} R_1 &= R, \quad R_2 = rR = rR_1, \\ C_1 &= C, \quad C_2 = C/\rho = C_1/\rho, \end{aligned} \quad (9)$$

and shown in Figure 2. Equations (9) are used in all design equations in this paper. Furthermore, from the expression for $\beta(r, \rho)$ in Table 2(b) it is seen that increasing the value of resistance ratio r , while keeping the value of capacitance ratio ρ equal to unity, the value of β is getting smaller and nearer to unity, and the term $(\beta-1)$ approaches zero, thus minimizing the influence of the $(\beta-1)$ -multiplied terms in (7).

Including the expression for $\beta(r, \rho)$ into sensitivities in (7) and with (9) we have the coefficient sensitivities in another form given by:

$$\begin{aligned} S_{R_1}^{a_1} &= q_p \left(\sqrt{\rho/r} + 1/\sqrt{\rho r}\right) - 1, \\ S_{R_2}^{a_1} &= -q_p \left(\sqrt{\rho/r} + 1/\sqrt{\rho r}\right), \\ S_{C_1}^{a_1} &= q_p \cdot \sqrt{\rho/r} - 1, \quad S_{C_2}^{a_1} = -q_p \cdot \sqrt{\rho/r}, \\ S_{R_G}^{a_1} &= S_{\beta}^{a_1} S_{R_G}^{\beta} = -S_{R_F}^{a_1} = q_p \left(\sqrt{\rho/r} + 1/\sqrt{\rho r}\right) - 1. \end{aligned} \quad (10)$$

Table 1. Transfer function coefficients of second-order active-RC filters with positive feedback in Fig. 2.

| Coefficient | (a) Low pass | (b) High pass | (c) Band pass -Type A |
|------------------------------|-----------------------------------------------------------------------|-----------------------------------------------------------------------|-----------------------------------------------------------------------|
| $a_0 = \omega_p^2$ | $(R_1 R_2 C_1 C_2)^{-1}$ | $(R_1 R_2 C_1 C_2)^{-1}$ | $(R_1 R_2 C_1 C_2)^{-1}$ |
| $a_1 = \frac{\omega_p}{q_p}$ | $\frac{R_1(C_1+C_2)+R_2C_2-\beta R_1C_1}{R_1 R_2 C_1 C_2}$ | $\frac{(R_1+R_2)C_2+R_1C_1-\beta R_2C_2}{R_1 R_2 C_1 C_2}$ | $\frac{R_2(C_1+C_2)+R_1C_1-\alpha\beta\cdot R_2C_1}{R_1 R_2 C_1 C_2}$ |
| K | $\alpha\beta$ | $\alpha\beta$ | $(1-\alpha)\beta q_p \sqrt{(R_2C_1)/(R_1C_2)}$ |
| Coefficient | (d) Band pass -Type B | (e) Band pass -Type A Dual | (f) Band pass -Type B Dual |
| $a_0 = \omega_p^2$ | $(R_1 R_2 C_1 C_2)^{-1}$ | $(R_1 R_2 C_1 C_2)^{-1}$ | $(R_1 R_2 C_1 C_2)^{-1}$ |
| $a_1 = \frac{\omega_p}{q_p}$ | $\frac{(R_1+R_2)C_2+R_1C_1-\alpha\beta\cdot R_2C_2}{R_1 R_2 C_1 C_2}$ | $\frac{R_2(C_1+C_2)+R_1C_1-\alpha\beta\cdot R_2C_1}{R_1 R_2 C_1 C_2}$ | $\frac{(R_1+R_2)C_2+R_1C_1-\alpha\beta\cdot R_1C_1}{R_1 R_2 C_1 C_2}$ |
| K | $(1-\alpha)\beta q_p \sqrt{(R_2C_2)/(R_1C_1)}$ | $(1-\alpha)\beta q_p \sqrt{(R_2C_1)/(R_1C_2)}$ | $(1-\alpha)\beta q_p \sqrt{(R_1C_1)/(R_2C_2)}$ |

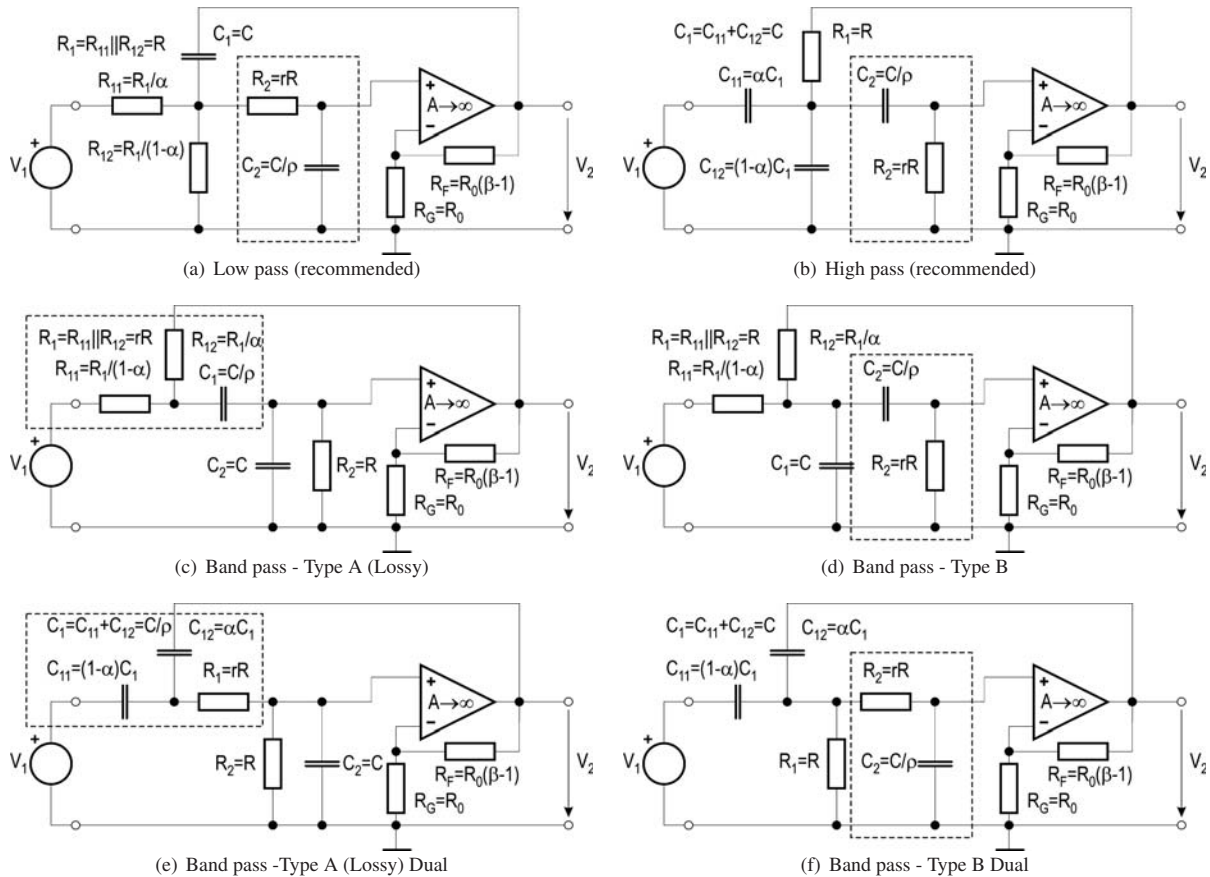


Fig. 2. Second-order active-RC filters with positive feedback and impedance scaling factors r and ρ

It can readily be seen that sensitivities in (10) are inversely proportional to the square root of r and partially proportional to the square root of ρ . (By *partial proportionality* we mean that ρ will appear partially in the numerator, partially in the denominator.)

Consequently, to reduce the sensitivity expressions, proportional quantities have to be decreased, those inversely proportional increased, and those partially proportional

should be equal to unity.

Thus, the sensitivities in (10) can be reduced by increasing the resistive scaling factor r while keeping the capacitive scaling factor ρ equal to unity. This will be the optimum strategy for desensitization of the HP filter to passive component tolerances (it is referred to as *partial tapering of the resistors* or *resistive tapering*). The high-impedance RC section is marked by the rectangle in Fig-

Table 2. Step-by-step design procedures for the design of low-sensitivity second-order active-RC filters in Fig. 2.

| Step\Type | (a) Low pass | (b) High pass | (c) Band pass -Type A (Lossy) |
|----------------------|-------------------------------------------------------------------------------------------------------------------------------------------------------------------------------------------------------------------------------|-----------------------------------------------------------------------------------------------------------------------------------------------------------------------------------------------------------------------------|------------------------------------------------------------------------------------------------------------------------------------------------------------------------------------------------------------------------------|
| i) Start | Choose: $C_1=1, \rho \gg 1$ (e.g. $\rho=4$) | Choose: $C_1=1, r \gg 1$ (e.g. $r=4$) | Choose: $C_2=1, \rho=1$ |
| ii) min. GSP | Choose: $r=1$ or r for min GSP $r = \frac{\rho}{36q_p^2} \times$ $\times \left[\sqrt{1 + 12q_p^2 \left(1 + \frac{1}{\rho}\right)} + 1 \right]^2$ | Choose: $\rho=1$ or ρ for min GSP $\rho = \frac{r}{36q_p^2} \times$ $\times \left[\sqrt{1 + 12q_p^2 \left(1 + \frac{1}{r}\right)} + 1 \right]^2$ | Choose: $r=\rho$ or r for min GSP $r = \frac{\rho}{36q_p^2} \times$ $\times \left[\sqrt{1 + 12q_p^2 \left(1 + \frac{1}{\rho}\right)} + 1 \right]^2$ |
| iii) ω_p, R_1 | $R_1 = \frac{1}{\omega_p C_1} \sqrt{\frac{\rho}{r}}$ | $R_1 = \frac{1}{\omega_p C_1} \sqrt{\frac{\rho}{r}}$ | $R_2 = \frac{1}{\omega_p C_2} \sqrt{\frac{\rho}{r}}$ |
| iv) GSP | $q_p \beta^2 \sqrt{\frac{\rho}{r}}$ | $q_p \beta^2 \sqrt{\frac{r}{\rho}}$ | $q_p \alpha \beta^2 \sqrt{\frac{1}{r\rho}}$ |
| v) β | $\beta = 1 + \frac{1+r}{\rho} - \frac{1}{q_p} \sqrt{\frac{r}{\rho}}$ | $\beta = 1 + \frac{1+r}{r} - \frac{1}{q_p} \sqrt{\frac{\rho}{r}}$ | $\alpha\beta = 1 + \rho + r - \frac{1}{q_p} \sqrt{\rho r}$ |
| vi) Components | $R_2 = rR_1; C_2 = C_1/\rho;$ $\alpha = K/\beta;$ $R_{11} = R_1/\alpha;$ $R_{12} = R_1/(1 - \alpha);$ $R_G = 1;$ $R_F = R_G(\beta - 1).$ | $R_2 = rR_1; C_2 = C_1/\rho;$ $\alpha = K/\beta;$ $C_{11} = \alpha C_1;$ $C_{12} = (1 - \alpha)C_1;$ $R_G = 1;$ $R_F = R_G(\beta - 1).$ | $R_1 = rR_2; C_1 = C_2/\rho;$ $R_G = 1;$ $\beta = (\alpha\beta) + 1/q_p \sqrt{r\rho} \cdot K;$ $\alpha = (\alpha\beta)/\beta;$ $R_{11} = R_1/(1 - \alpha);$ $R_{12} = R_1/\alpha;$ $R_F = R_G(\beta - 1).$ |
| Step\Type | (d) Band pass -Type B | (e) Band pass -Type A (Lossy) Dual | (f) Band pass -Type B Dual |
| i) Start | Choose: $C_1=1, r \gg 1$ (e.g. $r=4$) | Choose: $C_2=1, \rho=1$ | Choose: $C_1=1, \rho \gg 1$ (e.g. $\rho=4$) |
| ii) min. GSP | Choose: $\rho=1$ or ρ for min GSP $\rho = \frac{r}{36q_p^2} \times$ $\times \left[\sqrt{1 + 12q_p^2 \left(1 + \frac{1}{r}\right)} + 1 \right]^2$ | Choose: $r=\rho$ or r for min GSP $r = \frac{\rho}{36q_p^2} \times$ $\times \left[\sqrt{1 + 12q_p^2 \left(1 + \frac{1}{\rho}\right)} + 1 \right]^2$ | Choose: $r=1$ or r for min GSP $r = \frac{\rho}{36q_p^2} \times$ $\times \left[\sqrt{1 + 12q_p^2 \left(1 + \frac{1}{\rho}\right)} + 1 \right]^2$ |
| iii) ω_p, R_1 | $R_1 = \frac{1}{\omega_p C_1} \sqrt{\frac{\rho}{r}}$ | $R_2 = \frac{1}{\omega_p C_2} \sqrt{\frac{\rho}{r}}$ | $R_1 = \frac{1}{\omega_p C_1} \sqrt{\frac{\rho}{r}}$ |
| iv) GSP | $q_p \alpha \beta^2 \sqrt{\frac{r}{\rho}}$ | $q_p \alpha \beta^2 \sqrt{\frac{1}{r\rho}}$ | $q_p \alpha \beta^2 \sqrt{\frac{\rho}{r}}$ |
| v) β | $\alpha\beta = 1 + \frac{1+r}{r} - \frac{1}{q_p} \sqrt{\frac{\rho}{r}}$ | $\alpha\beta = 1 + \rho + r - \frac{1}{q_p} \sqrt{\rho r}$ | $\alpha\beta = 1 + \frac{1+r}{\rho} - \frac{1}{q_p} \sqrt{\frac{r}{\rho}}$ |
| vi) Components | $R_2 = rR_1; C_2 = C_1/\rho;$ $R_G = 1;$ $\beta = (\alpha\beta) + 1/q_p \sqrt{\rho/r} \cdot K;$ $\alpha = (\alpha\beta)/\beta;$ $R_{11} = R_1/(1 - \alpha);$ $R_{12} = R_1/\alpha;$ $R_F = R_G(\beta - 1).$ | $R_1 = rR_2; C_1 = C_2/\rho;$ $R_G = 1;$ $\beta = (\alpha\beta) + 1/q_p \sqrt{r\rho} \cdot K;$ $\alpha = (\alpha\beta)/\beta;$ $C_{11} = (1 - \alpha)C_1;$ $C_{12} = \alpha C_1;$ $R_F = R_G(\beta - 1).$ | $R_2 = rR_1; C_2 = C_1/\rho;$ $R_G = 1;$ $\beta = (\alpha\beta) + 1/q_p \sqrt{r/\rho} \cdot K;$ $\alpha = (\alpha\beta)/\beta;$ $C_{11} = (1 - \alpha)C_1;$ $C_{12} = \alpha C_1;$ $R_F = R_G(\beta - 1).$ |

ure 2(b). The investigations of coefficient sensitivities have been performed on all filter sections in this paper, but because of the lack of space, those expressions are not presented here. Only the results are used to present the optimum design strategies for each section.

If we consider, for example, the LP filter section in Figure 2(a) and calculate the a_1 -sensitivities then it will be shown that the desensitization is obtained in a dual way by increasing the value of capacitance ratio ρ while keeping the resistance ratio r equal to unity. This is because the LP and HP filter sections are RC-CR dual, and the positions of r and ρ simply exchange. This is true for all dual circuits. For every circuit in Figure 2, the optimum design procedure is summarized in Table 2.

Special cases are the BP-Type A Lossy and BP-Type A Lossy Dual circuits shown in Figure 2(c) and (e), respectively, that have the first RC sections with larger impedance (r and ρ are larger than or equal to unity). Those circuits can be constructed by the so-called Lossy LP-BP transformation [5]. It is shown in [5] and repeated here in Table 2, that optimum designs of those sections are those having equal ratios of capacitors and resistors.

3.2 Second-order sections with negative feedback

Consider the second-order filters shown in Figure 3, having ladder-RC network in an op-amp negative feedback. Transfer function coefficients are in Table 3. The voltage gain $\bar{\beta}$ is given by

$$\bar{\beta} = 1 + R_G/R_F. \quad (11)$$

Note that the gains β in (6) and $\bar{\beta}$ in (11) are connected by the complementary transformation and they are related

$$1/\bar{\beta} + 1/\beta = 1. \quad (12)$$

Furthermore, the circuits having negative feedback shown in Figure 3 are related to theirs counterparts in Figure 2 by the complementary transformation in [10].

The complementary transformation provides that all complementary circuits possess identical transfer functions with the same coefficients but with β and $\bar{\beta}$ interchanged (compare coefficients in Tables 1 and 3). This provides the same sensitivity characteristics and the *same design strategies* for complementary pairs [2]. For example, for both (+) BP-Type B filter in Figure 2(d) and (–) BP-Type R filter in Figure 3(d) there is the same optimum design procedure choosing $r > 1$ and $\rho = 1$ (or ρ for min. GSP) because they form one *complementary pair*. The complementary pairs are: {(+) HP, (–) BP-R}, {(+) LP, (–) BP-C}, {(+) LP, (–) BP-C}, {(+) BP-A-Lossy, (–) BP-Lossy}, {(+) BP-A-Lossy Dual, (–) BP-Lossy Dual}, {(+) BP-Type B, (–) BP-Type R} where (+) denotes positive feedback circuits and (–) circuits with negative feedback.

As shown above, there also exist *dual* circuits that possess *dual (opposite) design strategies*: those are the *dual pairs*: {(+) LP, (+) HP}, {(–) LP, (–) HP}, {(+) BP-A-Lossy, (+) BP-A-Lossy Dual}, {(–) BP-Lossy, (–) BP-Lossy Dual}, {(+) BP-B, (+) BP-B Dual}, {(–) BP-R, (–) BP-C}.

Note that complementary circuits form pairs between different feedbacks positive (+) and negative (–) types but the dual circuits in pair share the same feedback, i.e. positive (+) or negative (–).

For every circuit in Figure 3, the optimum design procedures are summarized in Table 4. The high-impedance sections are surrounded by dashed rectangle. Special cases are the *BP-Type Lossy* and *BP-Type Lossy Dual*. It is shown in Table 4, that optimum designs of those sections are those having equal ratios of capacitors and resistors.

Note that negative-feedback LP and HP filters in Figures 3(a)–(b) have gain-dependent a_0 and therefore are not preferable to use and have no equation for minimum GSP.

To design sections with low pole Q-factor, q_p (e.g. $q_p < 2$) unity gain *low-Q* version of the circuits can be used [8]. This is possible for all presented circuits except BP-Lossy and BP-Lossy Dual circuits in Figures 3(c) and (f), respectively. Those circuits are unable to realize pole Q-factor, $q_p \geq 0.5$ if they possess the unity gain $\bar{\beta} = 1$.

4 THIRD-ORDER BITRIPLETS

In this paper we consider two examples of the third-order filters with positive feedback [1, 3]. Those are the LP and HP filters, shown in Figure 4(a) and (b), respectively. The corresponding coefficients are given in Table 5. They are *RC-CR* duals of each other and from the optimum design of the LP circuit readily follow (*dual*) optimum design of the HP circuit. Optimum step-by-step design procedures are summarized in Table 6. In what follows we demonstrate our new design procedures on examples.

5 DESIGN EXAMPLES

5.1 Design of low-pass filters

Suppose we build an anti-aliasing LP filter, which is required to suppress high frequency components before sampling (compact disc recording device). The LP filter has to be as simple as possible (therefore we realize it using an active-RC filter), and must be selective. Because relatively high filter order is needed, the filter must have acceptably small sensitivity to component tolerance to be realizable without subsequent need for tuning. For those reasons we decided to use the cascade of optimized second- and/or one third-order allpole LP filter circuits presented in Figures 2(a) and 4(a).

In the example we will use the *cookbook* with closed form step-by-step design in Tables 2(a) and 6(a).

A LP filter has to satisfy the following specifications: the maximum pass-band attenuation of $A_{max} = 0.5$ dB for the frequencies up to the $f_p = 20$ kHz, and the minimum stop-band attenuation of $A_{min} = 50$ dB for the frequencies above $f_s = 34$ kHz. The filter has a unity gain in the pass band ($K = 1$). The normalized LP prototype cut-off frequency is $\Omega_s = f_s/f_p = 1.7$.

Using equations in [11] we can readily calculate the filter order n and the cut-off frequency ω_0 for the design of the Butterworth or Chebyshev filters. We have the following two solutions: *i*) Butterworth $n = 13$, $\omega_0 = 136253$ rad/s and *ii*) Chebyshev $n = 7$, $\omega_0 = 125664$ rad/s.

Note that the order n of the Chebyshev filters is smaller than the order of the Butterworth filter. Also recall that the Chebyshev filter with higher ripple would require lower filter order. Consequently, in what follows we realize the Chebyshev filter with 0.5 dB pass-band ripple.

The normalized Chebyshev poles readily follow from tables (e.g. in [8]) or using Matlab program. They are given by (and also shown in Figure 5):

$$\begin{aligned} p_0 &= -\sigma_0 = -0.25617 \\ p_1, p_1^* &= \sigma_1 \pm j\Omega_1 = -0.0570032 \pm j1.00641 \\ p_2, p_2^* &= \sigma_2 \pm j\Omega_2 = -0.159719 \pm j0.807077 \\ p_3, p_3^* &= \sigma_3 \pm j\Omega_3 = -0.230801 \pm j0.447894 \end{aligned} \quad (13)$$

Table 3. Transfer function coefficients of second-order active-RC filters with negative feedback in Fig. 3.

| Coefficient | (a) Low pass | (b) High pass | (c) Band pass -Type Lossy |
|------------------------------|--------------------------------------------------------------------|--------------------------------------------------------------------|--------------------------------------------------------------------|
| $a_0 = \omega_p^2$ | $[1 - (1 - \alpha)\beta]/(R_1 R_2 C_1 C_2)$ | $\{R_1 R_2 C_1 C_2 [1 - (1 - \alpha)\beta]\}^{-1}$ | $(R_1 R_2 C_1 C_2)^{-1}$ |
| $a_1 = \frac{\omega_p}{q_p}$ | $\frac{(R_1 + R_2)C_2 + R_1 C_1 - \beta R_1 C_1}{R_1 R_2 C_1 C_2}$ | $\frac{R_2(C_1 + C_2) + R_2 C_2 - \beta R_2 C_2}{R_1 R_2 C_1 C_2}$ | $\frac{R_2(C_1 + C_2) + R_1 C_1 - \beta R_2 C_1}{R_1 R_2 C_1 C_2}$ |
| K | $(1 - \alpha)\beta/[1 - (1 - \alpha)\beta]$ | $(1 - \alpha)\beta/[1 - (1 - \alpha)\beta]$ | $\alpha\beta q_p \sqrt{(R_2 C_1)/(R_1 C_2)}$ |
| Coefficient | (d) Band pass -Type R | (e) Band pass -Type C | (f) Band pass -Type Lossy Dual |
| $a_0 = \omega_p^2$ | $(R_1 R_2 C_1 C_2)^{-1}$ | $(R_1 R_2 C_1 C_2)^{-1}$ | $(R_1 R_2 C_1 C_2)^{-1}$ |
| $a_1 = \frac{\omega_p}{q_p}$ | $\frac{(R_1 + R_2)C_2 + R_1 C_1 - \beta R_2 C_2}{R_1 R_2 C_1 C_2}$ | $\frac{R_1(C_1 + C_2) + R_2 C_2 - \beta R_1 C_1}{R_1 R_2 C_1 C_2}$ | $\frac{R_2(C_1 + C_2) + R_1 C_1 - \beta R_2 C_1}{R_1 R_2 C_1 C_2}$ |
| K | $\alpha\beta q_p \sqrt{(R_2 C_2)/(R_1 C_1)}$ | $\alpha\beta q_p \sqrt{(R_1 C_1)/(R_2 C_2)}$ | $\alpha\beta q_p \sqrt{(R_2 C_1)/(R_1 C_2)}$ |

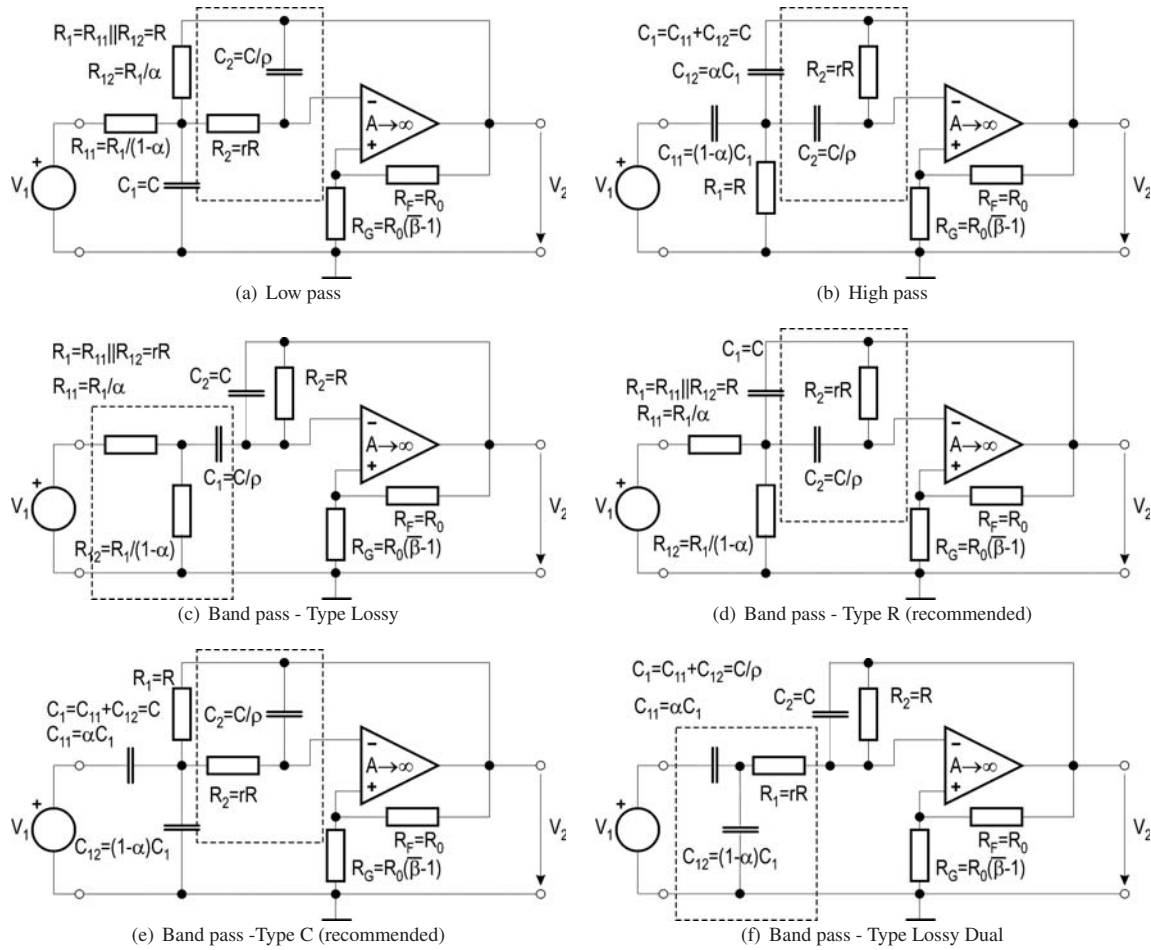


Fig. 3. Second-order active-RC filters with negative feedback and impedance scaling factors r and ρ

The corresponding normalized pole parameters are $\omega_{p1}=1.00802$, $q_{p1}=8.8418$ (max. Q), $\omega_{p2}=0.82273$, $q_{p2} = 2.575546$ (mid. Q), and $\omega_{p3}=0.503863$, $q_{p3} = 1.091552$ (min. Q). The resulting transfer function is:

$$T(s) = \frac{k}{(s+0.25617)(s^2+0.114006s+1.01611)} \times \frac{0.0447309}{(s^2+0.3194s+0.676884)(s^2+0.4616s+0.25388)} \quad (14)$$

In the even-order Chebyshev LP filter, the d.c. gain k

Table 4. Step-by-step design procedures for the design of low-sensitivity second-order active-RC filters in Fig. 3.

| Step\Type | (a) Low pass | (b) High pass | (c) Band pass -Type Lossy |
|----------------------|------------------------------------------------------------------------------------------------------------------------------------------------------------------------------------------|-----------------------------------------------------------------------------------------------------------------------------------------------------------------------------------------|-----------------------------------------------------------------------------------------------------------------------------------------------------------------------------------------|
| i) Start | Choose: $C_1=1, r=1, \rho \gg \gg$ (e.g. $\rho=4$) | Choose: $C_1=1, \rho=1, r \gg \gg$ (e.g. $r=4$) | Choose: $C_2=1, \rho=1, r=\rho$ or r for min GSP [see f) Type Lossy Dual] |
| ii) ω_p, R_1 | $R_1 = \frac{1}{\omega_p C_1} \sqrt{\frac{\rho}{r}} \cdot \frac{1}{\sqrt{K+1}}$ | $R_1 = \frac{1}{\omega_p C_1} \sqrt{\frac{\rho}{r}} \cdot \sqrt{K+1}$ | $R_2 = \frac{1}{\omega_p C_2} \sqrt{\frac{\rho}{r}}$ |
| iii) $\bar{\beta}$ | $\bar{\beta} = 1 + \frac{1+r}{\rho} - \frac{1}{q_p} \sqrt{\frac{r}{\rho}} \cdot \frac{1}{\sqrt{K+1}}$ | $\bar{\beta} = 1 + \frac{1+\rho}{r} - \frac{1}{q_p} \sqrt{\frac{\rho}{r}} \cdot \frac{1}{\sqrt{K+1}}$ | $\bar{\beta} = 1 + \rho + r - \frac{1}{q_p} \sqrt{\rho r}$ |
| iv) Components | $R_2 = rR_1; C_2 = C_1/\rho;$ $\alpha = 1 - K/[\bar{\beta}(K+1)];$ $R_{11} = R_1/(1-\alpha);$ $R_{12} = R_1/\alpha;$ $R_F = 1;$ $R_G = R_F(\bar{\beta}-1).$ | $R_2 = rR_1; C_2 = C_1/\rho;$ $\alpha = 1 - K/[\bar{\beta}(K+1)];$ $C_{11} = (1-\alpha)C_1;$ $C_{12} = \alpha C_1;$ $R_F = 1;$ $R_G = R_F(\bar{\beta}-1).$ | $R_1 = rR_2; C_1 = C_2/\rho;$ $\alpha = K/(\bar{\beta}q_p) \cdot \sqrt{r\rho};$ $R_{11} = R_1/\alpha;$ $R_{12} = R_1/(1-\alpha);$ $R_F = 1;$ $R_G = R_F(\bar{\beta}-1).$ |
| Step\Type | (d) Band pass -Type R | (e) Band pass -Type C | (f) Band pass -Type Lossy Dual |
| i) Start | Choose: $C_1=1, r \gg \gg$ (e.g. $r=4$) | Choose: $C_1=1, \rho \gg \gg$ (e.g. $\rho=4$) | Choose: $C_2=1, \rho=1$ |
| ii) min. GSP | Choose: $\rho=1$ or ρ for min GSP $\rho = \frac{r}{36q_p^2} \times$ $\times \left[\sqrt{1 + 12q_p^2 \left(1 + \frac{1}{r}\right)} + 1 \right]^2$ | Choose: $r=1$ or r for min GSP $r = \frac{\rho}{36q_p^2} \times$ $\times \left[\sqrt{1 + 12q_p^2 \left(1 + \frac{1}{\rho}\right)} + 1 \right]^2$ | Choose: $r=\rho$ or r for min GSP $r = \frac{\rho}{36q_p^2}$ $\times \left[\sqrt{1 + 12q_p^2 \left(1 + \frac{1}{\rho}\right)} + 1 \right]^2$ |
| iii) ω_p, R_1 | $R_1 = \frac{1}{\omega_p C_1} \sqrt{\frac{\rho}{r}}$ | $R_1 = \frac{1}{\omega_p C_1} \sqrt{\frac{\rho}{r}}$ | $R_2 = \frac{1}{\omega_p C_2} \sqrt{\frac{\rho}{r}}$ |
| iv) GSP | $q_p \bar{\beta}^2 \sqrt{\frac{r}{\rho}}$ | $q_p \bar{\beta}^2 \sqrt{\frac{\rho}{r}}$ | $q_p \bar{\beta}^2 \frac{1}{\sqrt{r\rho}}$ |
| v) $\bar{\beta}$ | $\bar{\beta} = 1 + \frac{1+\rho}{r} - \frac{1}{q_p} \sqrt{\frac{\rho}{r}}$ | $\bar{\beta} = 1 + \frac{1+r}{\rho} - \frac{1}{q_p} \sqrt{\frac{r}{\rho}}$ | $\bar{\beta} = 1 + \rho + r - \frac{1}{q_p} \sqrt{\rho r}$ |
| vi) Components | $R_2 = rR_1; C_2 = C_1/\rho;$ $\alpha = K/(\bar{\beta}q_p) \cdot \sqrt{\rho/r};$ $R_{11} = R_1/\alpha;$ $R_{12} = R_1/(1-\alpha);$ $R_F = 1;$ $R_G = R_F(\bar{\beta}-1).$ | $R_2 = rR_1; C_2 = C_1/\rho;$ $\alpha = K/(\bar{\beta}q_p) \cdot \sqrt{r/\rho};$ $C_{11} = \alpha C_1;$ $C_{12} = (1-\alpha)C_1;$ $R_F = 1;$ $R_G = R_F(\bar{\beta}-1).$ | $R_1 = rR_2; C_1 = C_2/\rho;$ $\alpha = K/(\bar{\beta}q_p) \sqrt{r\rho};$ $C_{11} = \alpha C_1;$ $C_{12} = (1-\alpha)C_1;$ $R_F = 1;$ $R_G = R_F(\bar{\beta}-1).$ |

Table 5. Transfer function coefficients of third-order active-RC filters with positive feedback in Fig. 4.

| Coefficient | (a) Low pass | (b) High pass |
|--------------------------------------------------|-------------------------------------------------------------------------------------------------------------------------------------------------------------------------------------|-----------------------------------------------------------------------------------------------------------------------------------------------------------------------------------|
| $a_0 = \gamma \omega_p^2$ | $\frac{1}{R_1 R_2 R_3 C_1 C_2 C_3}$ | $\frac{1}{R_1 R_2 R_3 C_1 C_2 C_3}$ |
| $a_1 = \omega_p^2 + \frac{\gamma \omega_p}{q_p}$ | $\frac{R_1 C_1 + (R_1 + R_2 + R_3) C_3 + (1-\beta) C_2 (R_1 + R_2)}{R_1 R_2 R_3 C_1 C_2 C_3}$ | $\frac{R_1 (C_1 + C_2) + R_2 (C_2 + C_3) + R_3 C_3 (1-\beta)}{R_1 R_2 R_3 C_1 C_2 C_3}$ |
| $a_2 = \gamma + \frac{\omega_p}{q_p}$ | $\frac{R_1 R_2 C_1 C_3 + R_1 R_3 C_3 (C_1 + C_2) + R_1 R_2 R_3 C_1 C_2 C_3}{R_1 R_2 R_3 C_1 C_2 C_3} + \frac{R_2 R_3 C_2 C_3 + (1-\beta) R_1 R_2 C_1 C_2}{R_1 R_2 R_3 C_1 C_2 C_3}$ | $\frac{R_1 R_2 C_1 (C_2 + C_3) + R_2 C_2 C_3 (R_1 + R_3) + R_1 R_2 R_3 C_1 C_2 C_3}{R_1 R_2 R_3 C_1 C_2 C_3} + \frac{R_1 R_3 C_3 (C_1 + C_2) (1-\beta)}{R_1 R_2 R_3 C_1 C_2 C_3}$ |
| K | $\alpha \beta$ | $\alpha \beta$ |

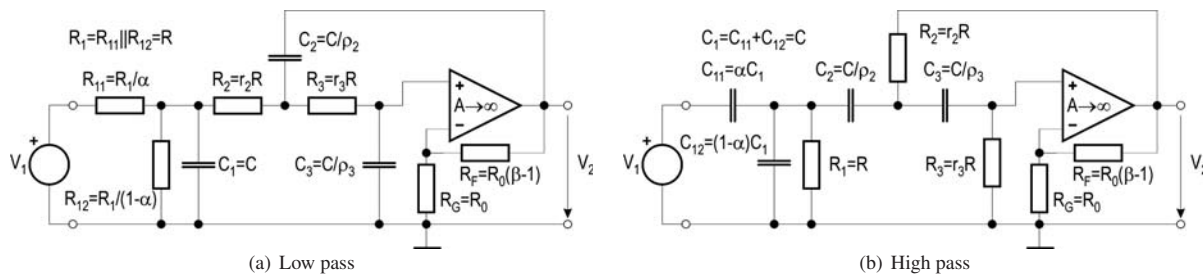


Fig. 4. Third-order active-RC filters with positive feedback and impedance scaling factors r_i and ρ_i ($i=2, 3$)

Table 6. Step-by-step design procedures for the design of low-sensitivity third-order active-RC filters in Fig. 4.

| Step\Type | (a) Low pass | (b) High pass |
|--------------------------------------------------------|-----------------------------------------------------------------------------------------------------------------------------------------------------------------------------------------------------------------------------------------|--------------------------------------------------------------------------------------------------------------------------------------------------------------------------------------------------------------------------------------------|
| i) Start | Choose: $\rho_2=\rho, \rho_3=\rho^2$ (e.g. $\rho=3$) | Choose: $r_2=r, r_3=r^2$ (e.g. $r=3$) |
| ii) Choose design frequency ω_0 | Choose: $\omega_0; \omega_0 < \omega_{0\max}$ where $\omega_0^3 - a_2\omega_0^2 + a_1\omega_0 - a_0 = 0 \rightarrow \omega_a$ $\omega_{DI} = 4a_0/(4a_1 - a_2^2)$ $\rightarrow \omega_{0\max} = \min\{\omega_a, \omega_{DI}\}$ | Choose: $\omega_0; \omega_{0\min} < \omega_0$ where $\omega_0^3 - a_2\omega_0^2 + a_1\omega_0 - a_0 = 0 \rightarrow \omega_a$ $\omega_{DI} = (4a_0a_2 - a_1^2)/4a_0$ $\rightarrow \omega_{0\min} = \max\{\omega_a, \omega_{DI}\}$ |
| iii) Normalize a_0, a_1, a_2 and calculate a, b, c | $\alpha_0 = a_0/\omega_0^3; \alpha_1 = a_1/\omega_0^2; \alpha_2 = a_2/\omega_0 \rightarrow$ $a = \alpha_0 + \alpha_2 - \alpha_1 - 1; b = \alpha_2 - 2;$ $c = -(1 + \rho_2).$ | $\alpha_0 = a_0/\omega_0^3; \alpha_1 = a_1/\omega_0^2; \alpha_2 = a_2/\omega_0 \rightarrow$ $a = \frac{1}{\alpha_0}(-\alpha_0 - \alpha_2 + \alpha_1 + 1); b = \frac{\alpha_1}{\alpha_0} - 2;$ $c = -(1 + r_2).$ |
| iv) Calculate r_2 (ρ_2) | $ar_2^2 + br_2 + c = 0 \rightarrow r_2$ (take positive and real r_2) | $a\rho_2^2 + b\rho_2 + c = 0 \rightarrow \rho_2$ (take positive and real ρ_2) |
| v) Calculate r_3 (ρ_3) | $r_3 = \rho_2\rho_3/(r_2\alpha_0)$ (In the step ii) above ω_0 should be chosen to provide $r_2 \approx r_3$ for min. sensitivity) | $\rho_3 = r_3r_2\alpha_0/\rho_2$ (In the step ii) above ω_0 should be chosen to provide $\rho_2 \approx \rho_3$ for min. sensitivity) |
| vi) β | $\beta = 1 + \frac{\rho_2}{\rho_3} - \frac{r_3}{\rho_3} \left[(\alpha_2 - 1) - \frac{1+\rho_2}{r_2} \right]$ | $\beta = 1 + \frac{r_2}{r_3} \left[\frac{\rho_3+r_3(1-\alpha_2)}{\rho_2+1} + 1 \right]$ |
| vii) Calculate R_1 | Choose: $C_1=1$, calculate $R_1 = (\omega_0 C_1)^{-1}$ | Choose: $C_1=1$, calculate $R_1 = (\omega_0 C_1)^{-1}$ |
| viii) Components | $C_2 = C_1/\rho_2; C_3 = C_1/\rho_3;$ $R_2 = r_2 R_1; R_3 = r_3 R_1;$ $\alpha = K/\beta; R_{11} = R_1/\alpha;$ $R_{12} = R_1/(1 - \alpha);$ $R_G = 1; R_F = R_G(\beta - 1).$ | $R_2 = r_2 R_1; R_3 = r_3 R_1;$ $C_2 = C_1/\rho_2; C_3 = C_1/\rho_3;$ $\alpha = K/\beta; C_{11} = \alpha C_1;$ $C_{12} = (1 - \alpha)C_1;$ $R_G = 1; R_F = R_G(\beta - 1).$ |

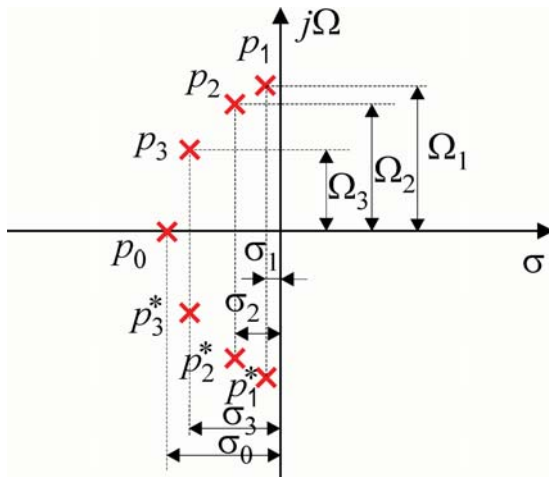


Fig. 5. Seventh-order 0.5dB Chebyshev filter pole plot

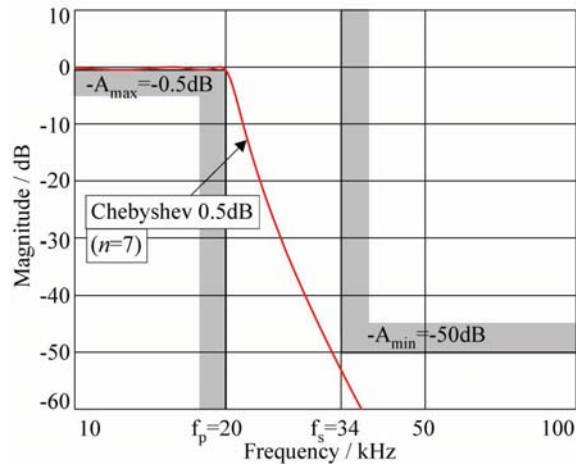


Fig. 6. The specifications and the Chebyshev LP filter transfer function magnitude

has to be equal to $-A_{max}$ [dB] providing the maximum magnitude 0 dB. In the odd-order Chebyshev LP filter we choose $k=1$, because the maximum magnitude is 0 dB at $\omega=0$ rad/s. The magnitude of the transfer function in (14) denormalized to $\omega_0 = 2\pi \cdot 20 \cdot 10^3$ rad/s is shown in Figure 6 together with filter specifications.

In what follows we present the design of each component in cascade (two biquads and one bitriplet). The first

design example is a mid-Q biquad with $q_{p2}=2.575546$ and $\omega_{p2}=0.822729$. The frequency ω_{p2} should be denormalized by multiplication with the pass-band cut-off frequency $\omega_0 = 2\pi \cdot 20 \cdot 10^3$ rad/s and the pole frequency for design $\omega_p=103387$ rad/s is obtained. The step-by-step design procedure of a second-order LP filter, shown in Figure 2(a), is in Table 2 column (a) and proceeds as follows:

i) For the LP filters most efficient is the capacitive tapering with equal resistors or resistor values for minimum GSP. Therefore we choose $\rho=4$ and $C_1=500\text{pF}$. Then we calculate: ii) $r=2.036$; iii) $R_1=27.1\text{k}\Omega$; and iv) $\text{GSP}=7.9287$. v) The gain $\beta=1.482$. From the last row vi) remaining components readily follow $R_2=55.21\text{k}\Omega$, $C_2=125\text{pF}$. For the unity gain $K=1$ the attenuation $\alpha=0.67476$, $R_{11}=40.18\text{k}\Omega$ and $R_{12}=83.37\text{k}\Omega$ follow. We choose $R_G=10\text{k}\Omega$; $R_F=4.82\text{k}\Omega$ follows. This design is recommended in this paper, because it is straightforward yielding an optimum biquad.

The expression for the GSP product in row iv) of Table 2 is given by:

$$\text{GSP} = \Gamma_A^{q_p} = A \cdot S_A^{q_p} = q_p \cdot \beta^2 \sqrt{\rho/r}. \quad (15)$$

Including the gain $\beta(r,\rho)$ into the $\text{GSP}(r,\rho)$ in (15), the latter has a minimum which can be found if we fix the value of ρ and set the first derivative to r equal to zero. The value of r which minimizes (15) is given by

$$r = \frac{\rho}{36q_p^2} \left[\sqrt{1 + 12q_p^2 \left(1 + \frac{1}{\rho}\right) + 1} \right]^2. \quad (16)$$

Equation (16) is in the row ii) in Table 2(a) in the form appropriate for the LP filter type. Because of duality between LP and HP filters the equation for min. GSP in the HP filter case, which is in the row ii) in Table 2 column (b), has the same form, but the start is with r and in a 'dual' way ρ is calculated.

There exists another ways on the design of LP filters, for example, with more emphasis to the reduction of passive

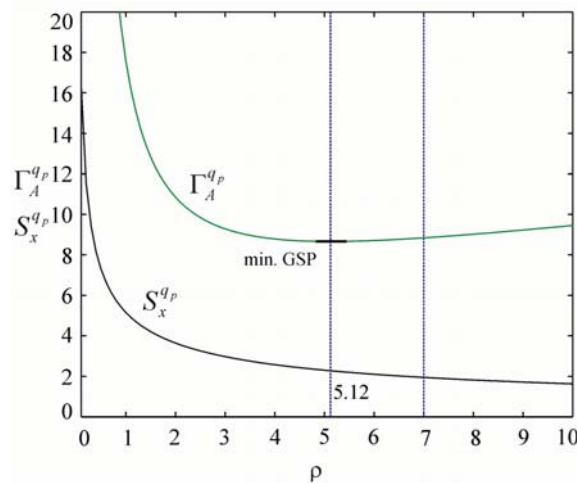


Fig. 7. Active and passive sensitivity plots for $q_p = 2.5755$

rather than active sensitivity. We can fix the value of r (e.g. by choosing equal resistors [$r=1$]: LP case) and then calculate ρ . Thus, there is a possibility to make derivative of (15) to ρ , that is, with given r we calculate ρ (which minimizes GSP in a different way) given by

$$\rho = \frac{r}{4q_p^2} \left[\sqrt{1 + 12q_p^2 \left(1 + \frac{1}{r}\right)} - 1 \right]^2. \quad (17)$$

The parameters using this alternative approach follow: $r=1$ (equal resistors); from (17) $\rho=5.121$ and $\text{GSP}=8.66$. Note that the GSP is slightly increased (worsen) but the passive sensitivity has decreased (improved) when compared to the above example.

The passive coefficient-to-component sensitivities for the LP filter have more or less the general form given by

$$S_x^{q_p} \approx q_p \cdot \left(\sqrt{\frac{r}{\rho}} + \frac{1}{\sqrt{r\rho}} \right), \quad (18)$$

where x represents any of the elements in the passive RC network. Both expressions for active (15) and passive (18) sensitivities having the value of r equal to unity and the value of ρ as an independent variable are plotted in Figure 7. It is shown in Figure 7 that the passive sensitivities decrease monotonically to zero with increasing value of ρ , while at the same time the active sensitivity has a minimum which can be found by (17). It can be seen that for a choice of ρ to the left of minimum both active and passive sensitivities increase rapidly. This is not appropriate because when $r=\rho=1$ (the simplest but not optimum design) there is high $\text{GSP}=17.57$, and the passive sensitivity is rather high. On the contrary, we see that GSP increases very slowly for ρ larger than 5.121 (min. GSP), whereas the value of passive sensitivity falls quite fast. Therefore, it is common practice to choose ρ somewhat larger than the value for minimum of GSP. For example, we could choose $r=1$ and $\rho=7$, which leads to $\text{GSP}=8.84$ and very low passive sensitivity.

We can conclude that the way in which we choose to design second-order filters is the trade off between passive and active sensitivities reduction.

The second design example is a min.-Q pole pair having $q_{p3} = 1.09155$ and $\omega_{p3} = 0.503863$, combined with the real pole $p_0 = \gamma = 0.25617$, to be realized by the third-order LP filter section in Figure 4(a). The frequencies ω_{p3} and γ are multiplied by the pass-band cut-off frequency $\omega_0 = 2\pi \cdot 20$ krad/s, and using the relations in the first column in Table 5, the denormalized coefficients of the third-order transfer function are given by

$$a_0 = 1.29057 \cdot 10^{14}, a_1 = 5.8764 \cdot 10^9, a_2 = 9.0198 \cdot 10^4. \quad (19)$$

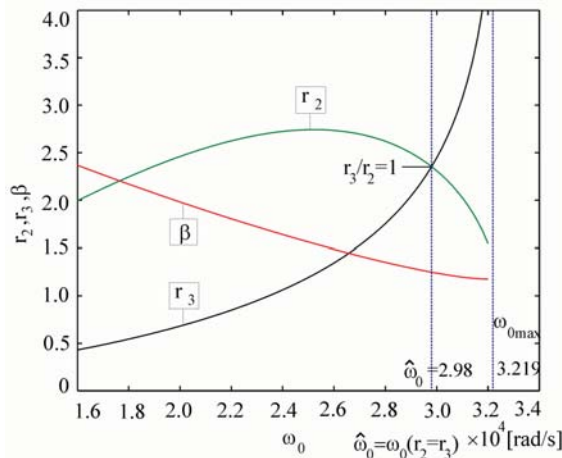


Fig. 8. Implicit and graphical method of finding ω_0 for the case $r_2 \approx r_3$ in third-order LP filter design

The step-by-step design procedure is in Table 6 column (a) and proceeds as follows:

i) Choose capacitive tapering: Select $\rho_2=3, \rho_3=9$. ii) Calculate ω_{0max} and select ω_0 for minimum sensitivity: From Table 6 line 2 $\omega_{DI}=33587\text{rad/s}$ and $\omega_a=32191\text{rad/s}$ are obtained; $\omega_{0max}=32191\text{rad/s}$. It is practical to draw all solutions for r_2, r_3 and β [calculated in the steps iv)–vi)] using Matlab as shown in Figure 8 and choose the value of the design frequency $\omega_0=2.98 \cdot 10^4$ rad/s, which will provide $r_2 \approx r_3$. This choice is consistent with the minimum sensitivity condition by the second-order LP filter: capacitive tapering with equal resistors ($\rho > 1, r = 1$). Note also that the value $\omega_0 < \omega_{0max}$ for the realizable filter.

iii) Calculate $\alpha_0, \alpha_1, \alpha_2$ and a, b and c : With $\omega_0 = 2.98 \cdot 10^4$, we obtain $\alpha_0=4.8768, \alpha_1=6.6173, \alpha_2=3.0268$, and therefore $a=0.28631, b=1.02678, c=-4$.

iv)–vi) Calculate r_2, r_3 and β : Solving the quadratic equation for r_2 , we obtain $r_2=2.3525$ and the values of $r_3=2.35342$ and $\beta=1.24797$ readily follow.

vii) Select C_1 and calculate remaining components: We choose $C_1=500\text{pF}$, thus $R_1=(\omega_0 C_1)^{-1}=67.1\text{k}\Omega$ and we obtain $C_2=167\text{pF}, C_3=55.5\text{pF}, R_2=157.886\text{k}\Omega$ and $R_3=157.95\text{k}\Omega$. Finally, for $K=1$ $\alpha=0.8013, R_{11}=83.76\text{k}\Omega, R_{12}=337.77\text{k}\Omega, R_G=10\text{k}\Omega$, and $R_F=2.48\text{k}\Omega$ are obtained. A simple check for the correctness of element values is to verify that $a_0=(R_1 R_2 R_3 C_1 C_2 C_3)^{-1}$. Element values for the seventh-order LP filter realized in cascade are summarized in Table 7. In the cascade the third-order biquad I realizes a real pole and a pole pair with min. Q combination, biquad II realized pole pair with mid. Q, and biquad III realizes max. Q poles. All biquads have unity pass-band gain K . For the purpose of sensitivity investigation, gain K

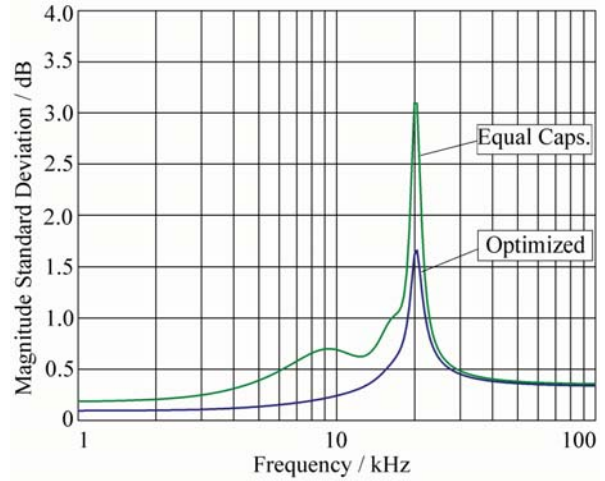


Fig. 9. Schoeffler sensitivities of the LP filter examples

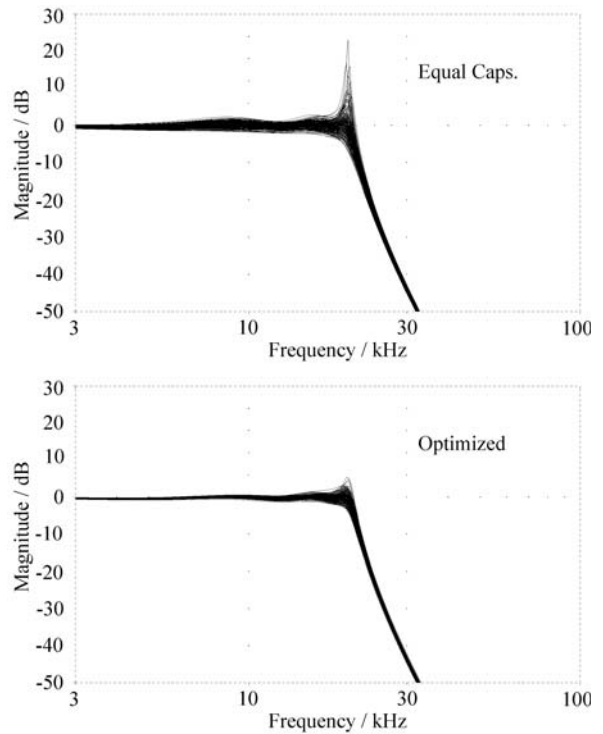


Fig. 10. MC runs of the LP filter examples

optimization for maximum dynamic range as in [12] is not needed.

Another *non-optimized* example (equal capacitors) of the seventh-order filter satisfying specifications in Figure 6 was calculated and the elements are presented in Table 7.

On both LP filter examples in Table 7 referred to as *Op-*

Table 7. Seventh-order LP filters elements (resistors in kΩ, capacitors in pF)

| | Biq. | R ₁₁ | R ₁₂ | R ₂ | R ₃ | C ₁ | C ₂ | C ₃ | R _G | R _F |
|-------------|------|-----------------|-----------------|----------------|----------------|----------------|----------------|----------------|----------------|----------------|
| Optimized | I | 83.75 | 337.8 | 157.9 | 157.9 | 500 | 167 | 55.5 | 10 | 2.48 |
| | II | 40.18 | 83.37 | 55.21 | | 500 | 125 | | 10 | 4.82 |
| | III | 38.4 | 62.28 | 41.97 | | 500 | 125 | | 10 | 6.17 |
| | Biq. | R ₁₁ | R ₁₂ | R ₂ | R ₃ | C ₁ | C ₂ | C ₃ | R _G | R _F |
| Equal Caps. | I | 190.9 | 173.6 | 48.60 | 14.04 | 500 | 500 | 500 | 10 | 11.00 |
| | II | 50.50 | 31.35 | 19.35 | | 500 | 500 | | 10 | 16.12 |
| | III | 45.58 | 24.2 | 15.79 | | 500 | 500 | | 10 | 18.87 |

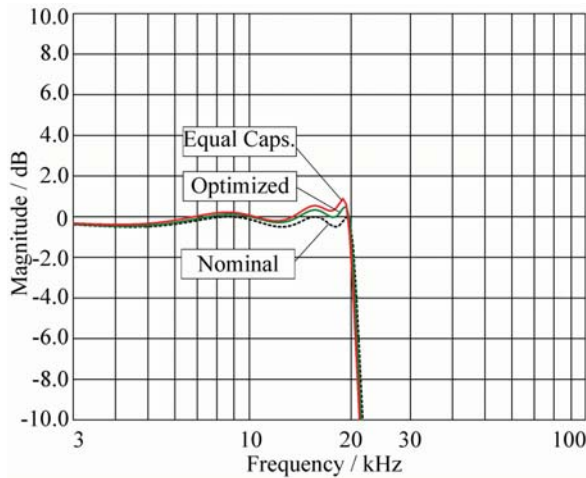


Fig. 11. Finite GBW influence on LP filter examples

timized and Equal Capacitors an overall sensitivity analysis was performed with the relative changes of the resistors and capacitors assumed to be uncorrelated random variables, with a zero-mean Gaussian distribution and 1% standard deviation. It was calculated the standard deviation $\sigma_\alpha(\omega)$ [dB] (which is related to the Schoeffler's sensitivities) of the variation of the logarithmic gain $\Delta\alpha=8.68588 \cdot \Delta|T(\omega)|/|T(\omega)|$ [dB], with respect to all passive elements, and the corresponding standard deviations $\sigma_\alpha(\omega)$ are shown in Figure 9. Monte Carlo (MC) runs using PSpice are shown in Figure 10 as a double check. It is demonstrated that the passive sensitivity is reduced by the optimum design using the cookbook presented in this paper.

An active sensitivity of seventh-order LP filter examples in Table 7 are investigated numerically using a single-pole model of the opamp response, given by

$$A(s) = \frac{A_0\omega_p}{s + \omega_p} = \frac{\omega_t}{s + \omega_p} \cong \frac{\omega_t}{s}, \quad (20)$$

where ω_t is the unity-gain bandwidth (the GBW product), A_0 the d.c. gain, and ω_p is the 3dB bandwidth. In the

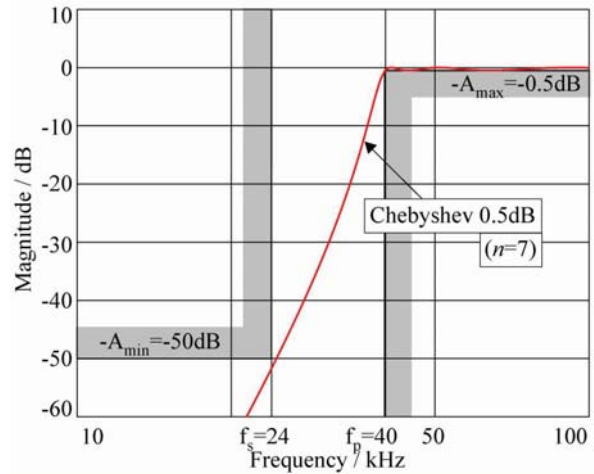


Fig. 12. The specifications and the Chebyshev HP filter transfer function magnitude

frequency range of interest, $\omega \gg \omega_p$, and we can assume $\omega_p=0$. To investigate influence of the real opamp, we incorporate $A(s)$ in (20) to the calculation of the overall filter's transfer function magnitude using Matlab. All simulations are done using element values from Table 7. One simulation is obtained with the constant gain $A(s)=A_0 \rightarrow \infty$ (nominal characteristic drawn by dotted line), while others use (20) with $\omega_t/(2\pi)=3\text{MHz}$, all shown in Figure 11. Observing Figure 11 one can conclude that the finite GBW product influence at high frequencies is reduced for the filter using optimized cascade (due to the GSP minimization) and much larger in the case of equal-capacitor (non-optimized) Biquads cascade. Note that for the third-order bitriplets there are no explicit equations for the GSP minimization as there were for the second-order biquads. Luckily, by the third-order sections, both active and passive sensitivities have been reduced at the same time.

5.2 Design of high-pass filters

An HP filter has to satisfy the specifications with the minimum stop-band attenuation of $A_{min}=50\text{dB}$ for the frequencies up to the $f_s=24\text{kHz}$, and the maximum pass-

Table 8. Seventh-order HP filters elements (resistors in kΩ, capacitors in pF)

| | Biq. | C_{11} | C_{12} | C_2 | C_3 | R_1 | R_2 | R_3 | R_G | R_F |
|------------|------|----------|----------|-------|-------|-------|-------|-------|-------|-------|
| Optimized | I | 400.6 | 99.43 | 212.7 | 212.4 | 1.887 | 5.660 | 16.98 | 10 | 2.482 |
| | II | 337.4 | 162.6 | 245.6 | | 4.671 | 18.68 | | 10 | 4.82 |
| | III | 309.3 | 190.7 | 283 | | 5.331 | 21.33 | | 10 | 6.166 |
| | Biq. | C_{11} | C_{12} | C_2 | C_3 | R_1 | R_2 | R_3 | R_G | R_F |
| Equal Res. | I | 33.35 | 36.58 | 129.7 | 451.6 | 10 | 10 | 10 | 10 | 10.97 |
| | II | 125.3 | 202. | 327.4 | | 10 | 10 | | 10 | 16.12 |
| | III | 138.9 | 262.1 | 401.1 | | 10 | 10 | | 10 | 18.87 |

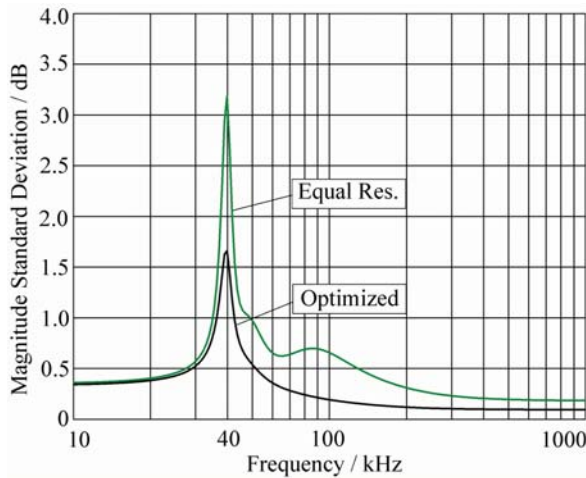


Fig. 13. Schoeffler sensitivities of the HP filter examples

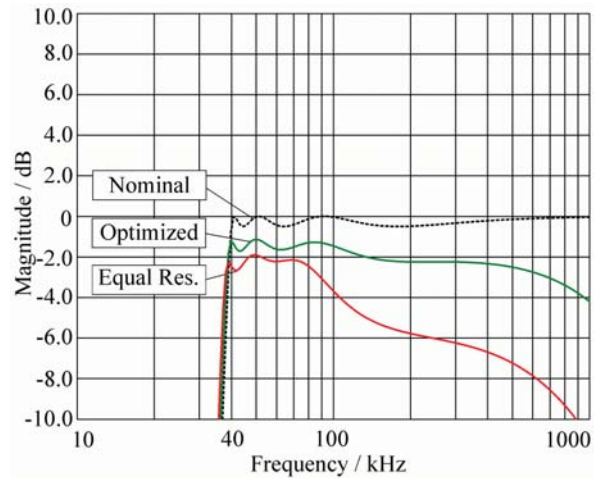


Fig. 14. Finite GBW influence on HP filter examples

band attenuation of $A_{max}=0.5\text{dB}$ for the frequencies above $f_p=40\text{kHz}$. Filter has a unity gain in the pass band. The normalized LP prototype cut-off frequency is $\Omega_s=f_p/f_s=1.67$. The specifications are met by the seventh-order 0.5dB Chebyshev filter.

In what follows we design HP filter with low sensitivity to component tolerances and reduced influence of the active component gain variation, which is very important to operate correctly on high frequencies. The cascade of optimized second- and/or one third-order allpole HP filter circuits as presented in Figures 2(b) and 4(b) is used. In the example the optimum design follows the closed form step-by-step equations in the Tables 2(b) and 6(b).

The Chebyshev poles in (13) are used. On the LP prototype normalized transfer function (14) we apply the LP-HP transformation

$$s_{LP} \rightarrow \omega_0/s, \tag{21}$$

where $\omega_0=2\pi \cdot f_p=251327 \text{ rad/s}$. According to (21) the frequency transformation yields new denormalized pole parameters $\omega_i=\omega_0/\omega_{iLP}$ ($i=1, 2, 3$) and $\gamma=\omega_0/\gamma_{LP}$ in [rad/s].

We obtain $\omega_{p1}=249327 \text{ rad/s}$, $q_{p1}=8.8418$ (max. Q), $\omega_{p2}=305480 \text{ rad/s}$, $q_{p2}=2.575546$ (mid. Q), and $\omega_{p3}=498801 \text{ rad/s}$, $q_{p3}=1.091552$ (min. Q) and $\gamma=981096 \text{ rad/s}$. The magnitude of the HP transfer function is shown in Figure 12 together with filter specifications. The *cookbook* design in this paper yields optimized filter sections. Filter components are given in Table 8. Note that the optimized Bitriple I has increasing resistor values and capacitors $C_2 \approx C_3$, which is the condition for the minimum sensitivity of HP filters (see row ν), column (b) in Table 6). Biquads II and III are designed in an optimum way with reduced passive sensitivity choosing $R_2=4R_1$ and capacitors ratio for min. GSP (reduced active sensitivity). This is a *dual* design to the LP filter.

Besides, a non-optimized filter sections are designed having equal resistors and components are given in Table 8, too. On both LP filter examples in Table 8 Schoeffler's sensitivities were calculated, and the corresponding standard deviations are shown in Figure 13.

All simulations for investigation of active sensitivities are done using element values from Table 8 and shown in Figure 14. Both Figures 13 and 14 demonstrate that the optimum designs recommended in this paper applied to filter

Table 9. Elements of the sixth-order BP filters with positive feedback (resistors in kΩ, capacitors in pF)

| | Biq. | R_{11} | R_{12} | R_1 | R_2 | C_1 | C_2 | R_G | R_F |
|------------|------|----------|----------|-------|-------|-------|-------|-------|-------|
| Optimized | I | 45.61 | 12.47 | 9.793 | 39.17 | 500 | 292.3 | 10 | 7.952 |
| | II | 36.27 | 7.195 | 6.004 | 24.02 | 500 | 265.1 | 10 | 8.656 |
| | III | 31.57 | 24.57 | 13.82 | 55.27 | 500 | 265.1 | 10 | 17.68 |
| | Biq. | R_{11} | R_{12} | R_1 | R_2 | C_1 | C_2 | R_G | R_F |
| Equal Res. | I | 76.22 | 16.06 | 13.26 | 13.26 | 500 | 500 | 10 | 20.0 |
| | II | 62.41 | 10.17 | 8.743 | 8.743 | 500 | 500 | 10 | 22.1 |
| | III | 51.59 | 32.98 | 20.12 | 20.12 | 500 | 500 | 10 | 35.25 |

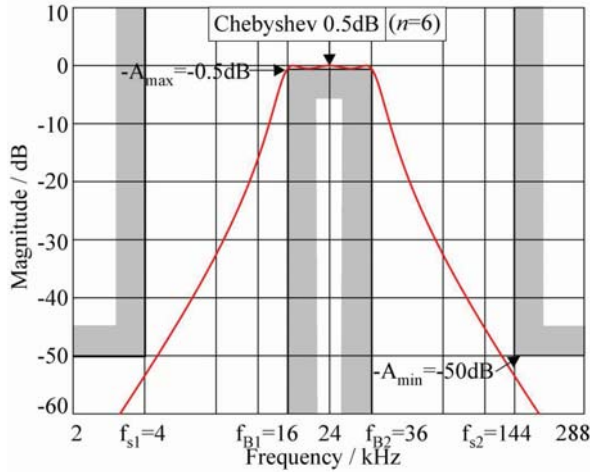


Fig. 15. The specifications and the Chebyshev BP filter transfer function magnitude

biquads yield low sensitivity filters (both passive and active sensitivities are reduced).

5.3 Design of band-pass filters

A BP filter has to satisfy the specifications with the minimum stop-band attenuation of $A_{min}=50\text{dB}$ for the frequencies up to the $f_{s1}=4\text{kHz}$, and above $f_{s2}=144\text{kHz}$ and the maximum pass-band attenuation of $A_{max}=0.5\text{dB}$ for the frequencies between $f_{B1}=16\text{kHz}$ and $f_{B2}=36\text{kHz}$. Central frequency of the filter $f_0 = \sqrt{f_{s1}f_{s2}} = \sqrt{f_{B1}f_{B2}} = 24\text{kHz}$, which shows that the filter is geometrically symmetrical with the band-width $B=2\pi \cdot (f_{B2}-f_{B1})=2\pi \cdot 20\text{krad/s}$. Filter has a unity gain in the pass band. The normalized LP prototype cut-off frequency is $\Omega_s=(f_{s2}-f_{s1})/(f_{B2}-f_{B1})=7$. The specifications are met by the sixth-order BP 0.5dB Chebyshev filter. The start is with the third-order LP prototype filter. The normalized poles using Matlab are:

$$p_0 = -\sigma_0 = -0.626456; \quad p_1, p_1^* = \sigma_1 \pm j\Omega_1 = -0.313228 \pm j1.02193. \quad (22)$$

The corresponding pole parameters are $\omega_{p1}=1.06885$, $q_{p1}=1.70619$ and $\gamma=0.626456$, and the resulting LP normalized transfer function is given by

$$T(s) = \frac{k \cdot 0.715694}{(s + 0.626456)(s^2 + 0.626456s + 1.14245)}. \quad (23)$$

On (23) we apply the LP-BP transformation

$$s_{LP} \rightarrow \frac{s^2 + \omega_0^2}{Bs}, \quad (24)$$

where $\omega_0=2\pi \cdot f_0$ and B are the BP parameters given above. We obtain the cascade realization of biquads with denormalized pole parameters of the BP filter

$$T(s) = \prod_{i=1}^3 \frac{k_i(\omega_{pi}/q_{pi})s}{s^2 + (\omega_{pi}/q_{pi})s + \omega_{pi}^2}, \quad (25)$$

where $\omega_{p1}=150796 \text{ rad/s}$, $q_{p1}=1.91554$, $k_1=1$, and using Geffe algorithm [13] $\omega_{p2}=228758 \text{ rad/s}$, $\omega_{p3}=99404.6 \text{ rad/s}$, $q_{p2}=q_{p3}=4.16858$, $k_2=1.87441$, and $k_3=7.35506$. (Note that the gains are optimized for maximum dynamic range [12].) The magnitude of the BP transfer function is shown in Figure 15 together with filter specifications. The *cookbook* design in Table 2(d) yields optimized Type B BP filter sections as in Figure 2(d). To all sections the same design strategy, which increases resistors ratios $r=R_2/R_1=4$ were applied, whereas the capacitors ratios $\rho=C_1/C_2$ were calculated for minimum GSP. Filter components are given in Table 9 for every biquad.

In the lower half of the same table there are elements of the non-optimized BP filter calculated by the simple design using equal resistors and equal capacitors. On both LP filter examples in Table 9 Schoeffler's sensitivities were calculated, and the corresponding standard deviations are shown in Figure 16. Symbol (+) indicate the filter circuits with positive feedback.

As the next example the filter was realized by a cascade of BP-Type R circuits as in Figure 3(d) with negative feedback (-). Those biquads are complementary to the biquads

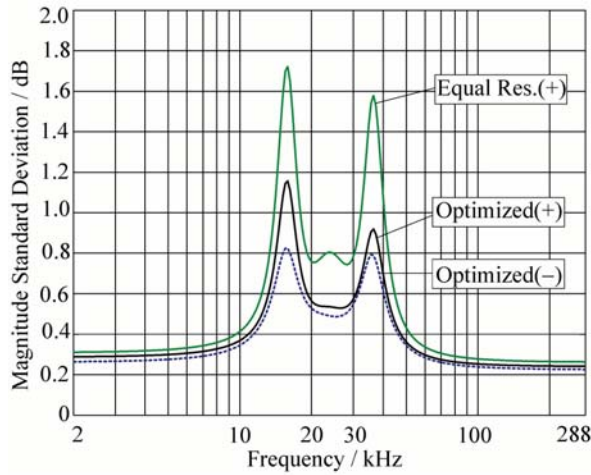


Fig. 16. Schoeffler sensitivities of the BP filter examples

in Figure 2(d). Elements of the complementary circuit (–) are calculated using the same design strategy as those for the (+) circuit ($r=4$ and ρ for min. GSP). The procedure in Table 4(d) is used and the same element values as R_1 , R_2 , C_1 and C_2 in Table 9 are obtained.

Or, in another, shorter way, we can start from elements R_1 , R_2 , C_1 and C_2 in Table 9 and recalculate attenuation $\bar{\alpha} = (1 - \alpha)/\alpha$, and gain $\beta = \alpha\beta$; the new $R_{11}=R_1/\bar{\alpha}$, $R_{12}=R_1/(1 - \bar{\alpha})$, $R_F=10k\Omega$ and $R_G=R_F(\bar{\beta}-1)$ follow.

The Schoeffler's sensitivity of that negative-feedback circuit (–) was calculated, as well, and shown in Figure 16 by dotted line. This circuit has the minimum sensitivity. The reason for that are more reduced sensitivities of a_1 to the resistors R_G , R_F in (–) circuits, and the absence of an additional sensitivities in a_1 (due to the feedback gain α) to the resistors R_{11} and R_{12} , when compared to (+) circuits.

All simulations for investigation of *active* sensitivities are done using element values from Table 9 and shown in Figure 17. Again the optimum designs presented in this paper applied to filter biquads yield low sensitivity filters. The optimized filter with (–) feedback has the magnitude nearest to the nominal (dotted) curve. This is because, for the same design parameters, the GSP product for (+) filter is $(1/\alpha) > 1$ times larger than that for the (–) filter (compare GSP equations in Tables 2(d) and 4(d)). Among all filters realizing BP transfer function the BP-Type R and his dual counterpart BP-Type C section in Figures 3(d) and (e), respectively, have the best performance.

6 CONCLUSIONS

In this paper we present an optimal design procedure for the most important second- and third-order active-RC

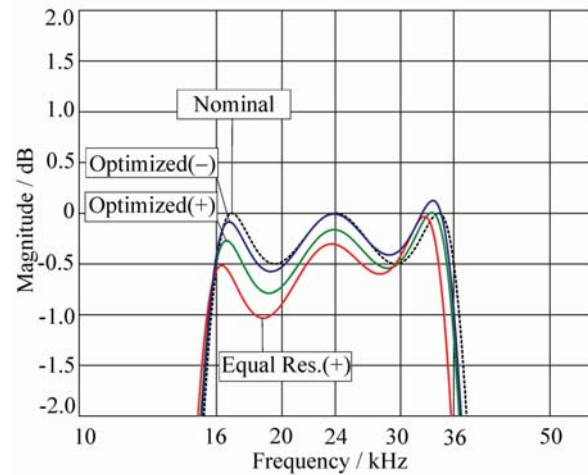


Fig. 17. Finite GBW influence on BP filter examples

single-amplifier building blocks in the form of a cookbook. The optimum design of the LP, HP and BP filters with positive and negative feedback is presented. The duality between filters and the complementary filters are investigated related to the optimum designs. Among all topologies the best (most useful) sections are indicated as *recommended*.

The new design provides optimum building blocks in a high-order filters having both passive and active sensitivity reduced compared to non-optimized simple designs. Some other design trade-offs that emphasizes more passive or active sensitivity reductions have been commented. Optimized sections can be used as building blocks in different filter structures such as cascade or multiple-feedback structures (e.g. *leap-frog* and *follow-the-leader-feedback*). A cascade design is the simplest one and using optimized second-order and/or third-order sections is the most practical and most useful solution in building higher-order filters.

The low passive sensitivity features, as well as the influence of the finite opamp's GBW product of the resulting circuits, are demonstrated on the high-order Chebyshev filter examples. The resulting low passive sensitivity is investigated using the Schoeffler sensitivity measure, whereas the low active sensitivity is shown using Matlab with real opamp parameters.

All calculations in the paper are done with denormalized parameters and elements, although the same equations can be used for calculations with normalized values.

REFERENCES

- [1] G. S. Moschytz, Low-Sensitivity, Low-Power, Active-RC Allpole Filters Using Impedance Tapering, *IEEE Trans. on Circuits and Systems*, vol. CAS-46(8), pp. 1009-1026, Aug. 1999.

- [2] D. Jurišić, G. S. Moschytz and N. Mijat, "Low-Sensitivity SAB Band-Pass Active-RC Filter Using Impedance Tapering", in Proc. of ISCAS 2001, (Sydney, Australia), Vol. 1, pp. 160-163, May 6-9, 2001.
- [3] D. Jurišić, *Active RC Filter Design Using Impedance Tapering*, Ph. D. Thesis, University of Zagreb, Croatia, April 2002.
- [4] D. Jurišić, G. S. Moschytz and N. Mijat, "Low-Sensitivity Active-RC High- and Band-Pass Second-Order Sallen and Key Allpole Filters," In Proc. of ISCAS 2002, (Phoenix, Arizona-USA), Vol. 4, pp. 241-244, May 26-29, 2002.
- [5] D. Jurišić, N. Mijat and G. S. Moschytz, "Optimal Design of Low-Sensitivity, Low-Power 2nd-Order BP Filters," in Proc. of ICSES 2008, (Krakow, Poland), pp. 375-378, September 14-17, 2008.
- [6] J. D. Schoeffler, The Synthesis of Minimum Sensitivity Networks, *IEEE Transactions on Circuit Theory*, pp. 271-276, June 1964.
- [7] R. P. Sallen and E. L. Key, A practical Method of Designing RC Active Filters, *IRE Trans. on Circuit Theory*, vol. CT-2, pp. 74-85, March 1955.
- [8] G. S. Moschytz and P. Horn, *Active Filter Design Handbook*, John Wiley&Sons, Chichester, 1981. (IBM Progr. Disk: ISBN 0471-915 43 2)
- [9] G. S. Moschytz, *Linear Integrated Networks: Design* (Bell Laboratories Series, New York: Van Nostrand Reinhold Co., 1975).
- [10] D. Hilberman, Input and Ground as Complements in Active Filters, *IEEE Trans. on Circuit Theory*, CT-20, pp. 540-547, September 1973.
- [11] D. Jurišić, G. S. Moschytz and N. Mijat, Low-Sensitivity, Single-Amplifier, Active-RC Allpole Filters Using Tables, *Automatika*, Vol. 49(3-4), pp. 159-173, Nov. 2008.
- [12] D. J. Perry, Scaling Transformation of Multiple-Feedback Filters, in Proc. IEE, vol.128, 176-179, Aug. 1981.
- [13] P. R. Geffe, Designer's Guide to Active Bandpass Filters, *EDN*, 46-52, April 5, 1974.



Dražen Jurišić is assistant professor of the Faculty of Electrical Engineering at the University of Zagreb in Croatia where he received his B.Sc., M.Sc. and Ph.D. degrees in Electrical Engineering in 1990, 1995 and 2002, respectively. In 2005 he was elected as assistant professor. He is involved in teaching lectures in undergraduate courses on "Electrical circuits", "Signals and systems" and "Analog and mixed signal processing circuitry". Present interests include analog and digital signal processing and filter design. He

worked as a researcher on the three scientific projects supported by Ministry of Science and Technology, Republic of Croatia. From 1997 until 1999 he was with Swiss Federal Institute of Technology (ETH) Zürich, Switzerland, as holder of Swiss Federal Scholarship for Foreign Students doing Ph.D. research in the field of analog active-RC filters. He was rewarded with the silver plaque "Josip Loncar" for his Ph.D. thesis. He is a member of KoREMA and IEEE-CAS society. He speaks English and German.



George S. Moschytz is head of the Electrical and Computer Engineering Department at the Bar-Ilan University in Israel. Present interests include analog and digital, sampled-data, and adaptive filters, for communication systems. Earlier Professor Moschytz was with RCA Labs in Zürich, Bell Telephone Labs, Holmdel, NJ, where he supervised a group designing analog and digital integrated circuits for data communications, and at ETH, Zürich, as Professor and Director of the Institute for Signal and Information Processing.

Author of "Linear Integrated Networks: Fundamentals" and "Linear Integrated Networks: Design", and co-author of the "Active Filter Design Handbook", and "Adaptive Filter" (in German). Editor of "MOS Switched-Capacitor Filters: Analysis and Design", and co-editor of "Tradeoffs in Analog Design". Authored many papers in the field of network theory, design, and analysis, and holds numerous patents in these areas. Professor Moschytz has held the position of president of the IEEE Circuit and Systems Society, and is an elected member of the Swiss Academy of Engineering Sciences. He is a Life-Fellow of the IEEE, and has received several IEEE awards, including the IEEE CAS Education Award.



Neven Mijat received his B.Sc., M.Sc. and Ph.D. degrees in Electrical Engineering from the Faculty of Electrical Engineering, University of Zagreb in 1970, 1974 and 1984, respectively. In 1970 he joined the Department of Electronic Systems and Information Processing at the Faculty of Electrical Engineering, University of Zagreb, where he is currently professor within the Networks, Systems and Signals group. At the Faculty he is involved in teaching lectures in undergraduate courses involving Network Theory, Filters, Analogue circuits, SC circuits, and in the postgraduate courses "Filter design", and "Numerical methods in system design". His current research interests include data acquisition systems and filter theory and realization methods. He was also leading a number of R&D projects. He is member of IEEE, CROMBES, KoREMA and some other professional societies. He was a principal investigator for few scientific projects and development projects for companies. He received the "Josip Loncar" silver plaques for his M.Sc. and Ph.D. theses in 1974 and 1984 respectively.

AUTHORS' ADDRESSES

Asst. Prof. Dražen Jurišić, Ph.D.

Prof. Neven Mijat, Ph.D.

**Faculty of Electrical Engineering and Computing,
University of Zagreb,**

Unska 3, HR-10000 Zagreb, Croatia

emails: drazen.juriscic@fer.hr, neven.mijat@fer.hr

Prof. George S. Moschytz, Ph.D.

School of Engineering,

Bar-Ilan University,

Ramat-Gan 52900, Israel

email: moschytz@isi.ee.ethz.ch

Received: 2009-08-04

Accepted: 2009-11-26